Toxicology Letters 232 (2015) 79–88

Contents lists available at ScienceDirect

Toxicology Letters

journal homepage: www.elsevier.com/locate/toxlet

Role of cytochrome P450-mediated metabolism and identification of novel thiol-conjugated metabolites in mice with phenytoin-induced liver injury

Eita Sasaki [a], Atsushi Iwamura [b], Koichi Tsuneyama [c], Tatsuki Fukami [a], Miki Nakajima [a], Toshiyuki Kume [b], Tsuyoshi Yokoi [a,d,*]

[a] Drug Metabolism and Toxicology, Faculty of Pharmaceutical Sciences, Kanazawa University, Kakuma-machi, Kanazawa, Ishikawa 920-1192, Japan
[b] DMPK Research Laboratories, Mitsubishi Tanabe Pharma Corporation, Kawagishi, Toda, Saitama 335-8505, Japan
[c] Department of Diagnostic Pathology, Graduate School of Medicine and Pharmaceutical Science for Research, University of Toyama, Sugitani, Toyama 930-0194, Japan
[d] Department of Drug Safety Sciences, Nagoya University Graduate School of Medicine, Tsurumai-cho, Showa-ku, Nagoya 466-8550, Japan

HIGHLIGHTS

- Role of P450-mediated metabolism in phenytoin (DPH)-induced liver injury was studied.
- Liver injury was exacerbated under the glutathione depletion in the DPH-mouse model.
- Novel glutathione-, *N*-acetylcysteine- and cysteine-conjugate of DPH were identified.
- Hepatic P450 levels correlated with those of plasma thiol conjugates levels.
- The arene oxide intermediate was suggested to involve in DPH-induced liver injury.

ARTICLE INFO

Article history:
Received 28 June 2014
Received in revised form 9 October 2014
Accepted 9 October 2014
Available online 18 October 2014

Keywords:
Hepatotoxicity
Glutathione
Cytochrome P450
Reactive metabolite
Phenytoin
Arene oxide

ABSTRACT

Phenytoin, 5,5-diphenylhydantoin (DPH), is widely used as an anticonvulsant agent. Severe hepatic injury rarely occurs in patients who received DPH. The development of liver injury is thought to be caused by reactive metabolites; however, the metabolites suggested to contribute to hepatotoxicity have not yet been detected *in vivo* and their effect on developing the liver injury is largely unknown. We recently demonstrated that DPH treatment decreased hepatic glutathione (GSH) contents, and GSH-depleted condition exacerbated DPH-induced liver injury in mice. The aim of the present study was to identify the reactive metabolite and to investigate the role of P450-mediated metabolisms in DPH-induced liver injury. We identified a novel GSH-conjugated (GS)-DPH, a conjugate of putative electrophilic arene oxide intermediate with GSH, in the bile of mice with DPH-induced liver injury. In plasma, cysteine- or *N*-acetylcysteine-conjugated DPH was detected, and these thiol conjugates levels were correlated with the plasma alanine aminotransferase (ALT) levels. These changes were significantly reduced by pretreatment with P450 inhibitor. Furthermore, the increases of hepatic P450 activities were in parallel with elevation of plasma thiol conjugates levels. These findings suggest that the arene oxide intermediate, which can be converted to thiol conjugates, is involved in DPH-induced liver injury.

Abbreviations: ABT, 1-aminobenzotriazole; ALT, alanine aminotransferase; BSO, L-buthionine-(S,R)-sulfoximine; Cys, cysteine; DPH, phenytoin; γ-GCS, γ-glutamilcysteine synthetase; 4′-HPPH, 5-(4′-hydroxyphenyl)-5-phenylhydantoin; MDZ, midazolam; NAC, *N*-acetylcysteine; TOL, tolbutamide.

* Corresponding author at: Department of Drug Safety Sciences, Nagoya University Graduate School of Medicine, 65 Tsurumai-cho, Showa-ku, Nagoya 466-8550, Japan. Tel.: +81 52 744 2110; fax: +81 52 744 2114.
E-mail addresses: esasaki@stu.kanazawa-u.ac.jp (E. Sasaki), iwamura.atsushi@mf.mt-pharma.co.jp (A. Iwamura), ktsune@med.u-toyama.ac.jp (K. Tsuneyama), tatsuki@p.kanazawa-u.ac.jp (T. Fukami), nmiki@p.kanazawa-u.ac.jp (M. Nakajima), kume.toshiyuki@mu.mt-pharma.co.jp (T. Kume), tyokoi@med.nagoya-u.ac.jp (T. Yokoi).

http://dx.doi.org/10.1016/j.toxlet.2014.10.012
0378-4274/

1. Introduction

Drug-induced liver injury is a serious issue for a new drug candidate as well as for marketed products. Phenytoin, 5,5-diphenylhydantoin (DPH), is widely used as an anticonvulsant drug. Few patients administered DPH will suffer symptoms of drug hypersensitivity, which is typically characterized by a rash, lymphadenopathy, fever, and hepatitis (Haruda, 1979). DPH-induced liver injury with a prominent inflammatory response occurs 1–8 weeks after exposure in approximately 1–1000 and 1–10,000 patients who receive DPH (Mullick and Ishak, 1980). Thus, DPH-induced liver injury is generally recognized as idiosyncratic. The molecular basis underlying this hypersensitivity, including the liver injury, has not been fully characterized, although it has been proposed that DPH can be bioactivated in response to reactive intermediates, which can undergo haptenization with normal proteins to generate neoantigens that elicit adverse reactions (Spielberg et al., 1981).

It has also been suggested that glutathione (GSH) modulates DPH metabolism by either trapping the DPH reactive intermediate and decreasing protein binding or by protecting proteins from attack *via* electrophilic or free radical intermediates of DPH (Roy and Snodgrass, 1990). Roy and Snodgrass (1988) demonstrated that the addition of thiols, *i.e.*, GSH, cysteine and cysteamine, significantly decreased covalent binding to rat or mouse microsomes. In addition, *in vivo* pretreatment with diethyl maleate, a well-known GSH depletion reagent, resulted in a significant increase in covalent binding of metabolites (Roy and Snodgrass, 1988). On the basis of these findings, it is likely that quinone or arene oxide intermediates, which could be detoxified *via* thiol conjugation, may be involved in DPH-induced liver injury *via* the formation of protein-drug adducts. However, thiol-drug conjugates of DPH have not yet been identified *in vitro* and *in vivo*.

A previous study has shown that DPH is a inducer of cytochrome P450 (CYP)2C and CYP3A in humans (Chaudhry et al., 2010; Fleishaker et al., 1995), rats (Yamazaki et al., 2001) and mice (Hagemeyer et al., 2010). On the basis of these findings, it is likely that modulation of P450-mediated metabolic activation of DPH may be involved in initiating DPH-induced liver injury.

Although, as described above, number of studies postulates the existing reactive metabolite in DPH metabolisms, there are lacking an evidence of *in vivo* hepatotoxicity. An animal model for drug-induced liver injury is critical in characterizing the relationship between reactive metabolites formation, development of liver injury, and immune reaction in the liver. Recently, we established a mouse model of DPH-induced liver injury in combination with L-buthionine-(S,R)-sulfoximine (BSO), a well-known GSH synthesis inhibitor, treatment (Sasaki et al., 2013). In our previous study, DPH-induced liver injury was exacerbated under GSH depleted conditions and these phenomena were suppressed using a non-selective P450 inhibitor, 1-aminobenzotriazole (ABT) in mice (Sasaki et al., 2013). Considering together, the reactive metabolite, which can be trapped by GSH, is most likely to involve the development of the hepatotoxicity.

The aim of the present study was to identify the reactive metabolite that contributes to the development of DPH-induced liver injury, presumably *via* GSH conjugates that are further metabolized *via* the mercapturic acid pathway. Furthermore, we analyzed the effects of P450 inhibitor on DPH-induced liver injury, changes in plasma thiol conjugate levels, hepatic GSH contents, and plasma alanine aminotransferase (ALT) levels in the DPH-induced liver injury mice.

2. Materials and methods

2.1. Materials

BSO and DPH were purchased from Wako Pure Chemical Industries (Osaka, Japan). ABT was purchased from the Tokyo Chemical Industry (Tokyo, Japan). Glucose 6-phosphate (G6P), glucose-6-phosphate dehydrogenase (G6PDH) and β-nicotinamide adenine dinucleotide phosphate, oxidized form, and monosodium salt ($NADP^+$) were obtained from Oriental Yeast (Tokyo, Japan). Anti-mouse Cyp3a monoclonal antibody (sc-30621) was obtained from Santa Cruz Biotechnology (Santa Cruz, CA). Anti-rat CYP2C13 polyclonal antibody, which cross-reacts with mouse Cyp2c, was obtained from Sekisui Medical (Ibaraki, Japan). Acetonitrile and methanol (Kanto Chemical, Tokyo, Japan) were of high performance liquid chromatography (HPLC) grade, and all other chemical reagents were of the highest grade commercially available.

2.2. Animal treatment

Female C57BL/6JmsSLC (8 weeks old, 16–21 g) were obtained from SLC Japan (Hamamatsu, Japan). The mice were housed in a controlled environment (temperature $23 \pm 1\,^{\circ}C$, humidity $50 \pm 10\%$, and 12 h light/12 h dark cycle) in the institution's animal facility with *ad libitum* access to food and water. The mice were acclimatized before use in the experiments. Animal maintenance and treatment were performed according to the National Institutes of Health Guide for Animal Welfare of Japan, and the protocols were approved by the Institutional Animal Care and Use Committee of Kanazawa University, Japan.

We generated DPH-induced liver injury in mice as previously described (Sasaki et al., 2013). Briefly, mice were intraperitoneally injected with DPH in corn oil at a dose of 50 mg/kg for 2 days followed by oral administration of 100 mg/kg on days 3 through 5. BSO dissolved in saline was intraperitoneally injected at a dose of 700 mg/kg for 1 h prior to DPH administration. Vehicle was used as a control. To determine the time-dependent changes in plasma ALT levels at 0, 1.5, 3, 6, 9, 12, and 24 h after the final DPH administration, blood was collected *via* the tail vein. The plasma ALT levels were measured using a Fuji Dri-Chem 4000 V (Fuji Film Med., Tokyo, Japan). To assess the concentration of DPH and its metabolites at 0, 1.5, 3, 6, 12, and 24 h after the DPH administration, or 0, 3, 6, 9, 12, and 24 h after the final DPH administration for the ABT co-administration study, blood was collected *via* the tail vein. The plasma concentration of DPH and its thiol conjugates were determined as described below.

2.3. Treatment of ABT

Mice were intraperitoneally injected with ABT (100 mg/kg in saline) 1 h prior to the final DPH administration as previously described (Sasaki et al., 2013; Shimizu et al., 2009; Mugford et al., 1992). Vehicle was used as a control.

2.4. GSH assay and histopathological analysis

At 0, 1.5, 3, 6, 12, and 24 h after the final DPH administration, blood was collected from the inferior vena cava for assessment of the plasma ALT levels. A portion of the hepatic left lobe was removed and fixed in 10% neutral buffered formalin for histopathological examination. The fixed liver specimens were trimmed, embedded in paraffin wax, sectioned at 4 μm thickness, and stained with hematoxylin and eosin (H&E) for microscopic examination. The remaining liver was frozen in liquid nitrogen, and stored at $-80\,^{\circ}C$ for GSH measurement. The mouse liver was

homogenized in ice-cold 5% sulfosalicylic acid and centrifuged at 8000 × *g* at 4 °C for 10 min. The total GSH and glutathione disulfide (GSSG) concentration in the supernatant was measured as previously described (Tietze, 1969). The GSH levels were calculated from the difference between the total glutathione (GSH + GSSG) and GSSG concentration.

2.5. Collection of bile

Animal surgery for the collection of bile was performed as previously reported (Kitamura et al., 2008) with slight modifications. Briefly, 3 h after the final administration of DPH, the mice were anesthetized with diethyl ether and a polyethylene cannula (PE-5; Eicom, Kyoto, Japan) was surgically placed into the common bile duct. Bile was collected until 6 h after the final DPH administration.

2.6. Characterization and determination of GSH-conjugated DPH, cysteine-conjugated DPH, and N-acetylcysteine-conjugated DPH adducts in plasma and bile

To identify GSH-conjugated DPH (GS-DPH), cysteine-conjugated DPH (Cys-DPH) and *N*-acetylcysteine-conjugated DPH (NAC-DPH) in plasma and bile, the optimized conditions were as follows: in plasma, 40 μl of acetonitrile was added to 20 μl of plasma and the mixture was centrifuged at 13,000 × *g* for 3 min. In bile, 20 μl of acetonitrile was added to an equal volume of bile and the mixture was centrifuged at 13,000 × *g* for 3 min. The supernatant was used for further analysis. Liquid chromatography–tandem mass spectrometry (LC–MS/MS) was performed using the HP1200HPLC system (Agilent) coupled to Q-TOF Ultima (Micromass). The column used was SunShell (2.6 μm, 150 mm × 2.1 mm I.D.). The elution conditions consisted of a gradient of ammonium formate (95–35% for 15 min, 35–5% for 2 min, 5–95% for 1 min, 95% for 7.9 min) in acetonitrile at flow rate of 0.2 ml/min. Electrospray ionization was performed with a source temperature of 120 °C and ion spray voltage of 2.8 kV and 3.2 kV in the positive and negative ion mode, respectively. Argon was used as the collision gas. The collision energy was 5 eV, cone voltage was 35 V, and desolvation temperature was 250 °C. Nitrogen was used as both the cone gas and desolvation gas. The cone gas and desolvation gas flow were set at 100 l/h and 800 l/h flow, respectively. To determine novel metabolites, data acquired using LC–Q-TOFMS were processed by MetaboLynx software (Waters). The structure of each novel DPH metabolites were elucidated using MS^2 fragmentation with collision energy ramping from 10 to 40 eV.

2.7. Comprehensive detection of plasma DPH and its thiol conjugates

To comprehensively detect of DPH, Cys-DPH, and NAC-DPH in plasma, 20 μl of acetonitrile and 200 μl of internal standard (IS) solution (0.01 μM of verapamil in methanol) was added to 5 μl of plasma, and the mixture was centrifuged at 13,000 × *g* for 3 min. The supernatant was used for further analysis. LC–MS/MS was performed using an Acquity HPLC system (Waters, Manchester, UK) coupled to a Waters Xevo TQ tandem quadrupole mass spectrometer (Micromass MS Technologies, Manchester, UK). The column was an Acquity UPLC BEH C18 column (1.7 μm, 30 mm × 1.1 mm I.D.; Waters, Milford, MA, USA). The elusion conditions consisted of a gradient of 10 mM ammonium formate (98% for 0.5 min, 80% for 1.1 min, 65% for 0.4 min, 2% for 0.5 min, 98% for 0.5 min) in acetonitrile at a flow rate of 0.5 ml/min. MS/MS data acquisition was performed with an electrospray source operating in the negative or positive mode (ESI_{neg} or ESI_{pos}) under multiple reaction monitoring (MRM) conditions as shown in Table 1. The optimized values for the Xevo TQ MS instrument were as follows; capillary voltage 0.5 kV; source temperature 150 °C; desolvantion temperature 600 °C. Nitrogen was used as both the cone gas and desolvation gas. The cone gas and desolvation gas flow were set at 100 l/h and 1200 l/h flow, respectively. Argon was used as collision gas with 0.15 ml/min flow. In the case of DPH, the plasma concentrations were calculated on the basis of a standard curve, and the thiol conjugates were determined from the peak area ratios of metabolite to the IS area as semi-quantitation because no standard compounds were available. DPH and its thiol conjugates were identified *via* an accurate mass measurement, comparison with authentic standards (DPH), and analysis of the tandem mass spectrometry (MS^2) fragmentation pattern.

Table 1
MS/MS optimized conditions for the Xevo TQ MS instrument.

Compound	Mass	MRM transition	Ion mode	CV (V)	CE (eV)
DPH	253.04	253.04 > 182.00	ES+	30	20
Cys-DPH	370.1	370.10 > 283.10	ES−	25	15
NAC-DPH	412.1	412.10 > 283.10	ES−	25	15
IS (verapamil)	455	455.00 > 165.00	ES+	40	30

Abbreviations: CE, collision energy; CV, cone voltage; Cys-, cysteine-conjugated; DPH, phenytoin; ES, electrospray source; IS, internal standard; MRM, multiple reaction monitoring; NAC-, N-acetylcysteine-conjugated.

2.8. Preparation of mouse liver microsomes

The mouse liver was prepared from each time point during repetitive administration of DPH. As previously described, the mice were intraperitoneally injected with DPH in corn oil at a dose of 50 mg/kg for 2 days followed by oral administration 100 mg/kg on days 3 through 5. BSO dissolved in saline was intraperitoneally injected at a dose of 700 mg/kg 1 h prior to DPH administration. During repetitive administration, on days 0, 1, 3, and 4, the liver of each mouse was immediately collected. Liver microsomes were prepared according to a previous study (Emoto et al., 2000).

2.9. Cyp2c and Cyp3a enzyme assays and immunoblot analyses

Tolbutamide (TOL) hydroxylation and midazolam (MDZ) 1′-hydroxylation activity of mouse liver microsomes, as probes of Cyp2c and Cyp3a enzyme activity, respectively, were determined according to a previous report (Emoto et al., 2000) with slight modifications. Briefly, the standard incubation mixture (final volume 0.2 ml) contained 1.0 mg/ml protein of mouse liver microsomes, 100 mM potassium phosphate buffer (pH 7.4), a nicotinamide adenine dinucleotide phosphate (NADPH)-generating system consisting of 0.5 mM $NADP^+$, 5 mM G6P, 0.5 unit/ml G6PDH and 5 mM $MgCl_2$, and 100 μM of each substrate. The reaction mixtures were incubated at 37 °C for 15 min for MDZ hydroxylation and 60 min for TOL hydroxylation. After deproteination, each hydroxylated metabolite was monitored using an HPLC system. SDS-polyacrylamide gel electrophoresis and immunoblot analysis were performed according to Laemmli (1970). Liver microsomes, 1 μg and 4 μg for Cyp2c and Cyp3a detection, respectively, were separated on 7.5% polyacrylamide gels and electrotransferred onto polyvinylidene difluoride membranes, Immobilon-P (Millipore, Billerica, MA). The membranes were probed with each of the antibodies and the corresponding fluorescent dye-conjugated secondary antibody. An Odyssey Infrared Imaging system (LI-COR Biosciences, Lincoln, NE) was used for the detection. The band intensity levels were quantified using ImageQuant TL Image Analysis software (GE Healthcare, Little Chalfont, Buckinghamshire, UK).

2.10. Statistical analysis

The data are shown as the mean ± SE. Statistical analyses of multiple groups were performed using one-way ANOVA with the Dunnett's *post hoc* test to determine the significance of the differences between individual groups. Comparisons between 2 groups were performed using a 2-tailed Student's *t*-test. A value of $p < 0.05$ was considered statistically significant.

3. Results

3.1. Time-dependent changes of plasma ALT levels, liver histopathology, and hepatic GSH contents in DPH-induced liver injury mouse model

According to a previous report (Sasaki et al., 2013), mice were intraperitoneally injected with DPH in corn oil at a dose of 50 mg/kg for 2 days followed by an oral administration 100 mg/kg on days 3 through 5. To deplete hepatic GSH, BSO, a γ-glutamylcysteine synthetase (γ-GCS) inhibitor, was intraperitoneally injected at a dose of 700 mg/kg 1 h prior to each DPH administration. After the final DPH treatment, the mice treated with both DPH and BSO showed a significant increase in plasma ALT levels compared to the DPH alone-treated mice (Fig. 1A), whereas DPH alone-treated mice showed mild increases in plasma ALT levels. The previous report indicate that on days 1 through 3, the plasma ALT levels were not significantly increased, and on day 4, the plasma ALT levels were significantly but not markedly increased compared with vehicle-treated mice (Sasaki et al., 2013). Consideration of this result, the liver injury is mainly occurred after the final DPH administration in this mouse model.

Histopathologically, apoptotic cells and ballooning cells were observed in mice treated with both DPH and BSO (Fig. 1B), whereas DPH alone-treated mice showed mild lipid droplets, but apoptosis or ballooning cells were not observed. In the BSO alone-treated mice, the hepatic GSH contents were significantly decreased at 3 h, whereas DPH and BSO co-administrated mice were significantly decreased at 6 h after the final DPH administration compared with 0 h mice (Fig. 1C). In addition, at 0 h and 24 h after the final DPH administration, DPH and BSO co-treatment significantly decreased the hepatic GSH contents compared with BSO alone-treated mice. These results indicated that DPH treatment consume hepatic GSH and the liver injury was exacerbated under the GSH-decreased condition.

3.2. Comprehensive detection and characterization of GS-DPH, Cys-DPH, and NAC-DPH adducts in bile and plasma

Generally, the direct detection of reactive metabolites of a drug is difficult due to its instability. The results from the DPH-induced liver injury exacerbated by the GSH-depleted condition (Fig. 1A), revealed that the hepatotoxic reactive metabolite derived from DPH could be trapped by GSH, thereby contributing to the detoxification of reactive metabolites. Thus, we attempted to detect the thiol-conjugated metabolites in DPH-induced liver injury in mice. GS-, Cys-, and NAC-adducts, as putative stable products of the electrophilic metabolites, were examined using LC–MS/MS analysis in bile and plasma. Animals were not treated with BSO because GSH depletion causes difficulty in detecting its conjugates.

In bile, GS-DPH adduct (m/z 556) was detected and the ion chromatogram showed a peak at 9.87 min of elution time. The MS spectrum of eluent included m/z 556 $[M-H]^-$ of GS-DPH adducts (Fig. 2A). The mass of the molecular ion of GS-DPH (m/z 556) suggested an addition of 305 Da to the mass of DPH (m/z 251), which corresponded to the addition of GS-molecules (305 Da) to the DPH mass (Fig. 2A). The MS^2 spectrum of GS-DPH showed a characteristic loss of 129 amu (corresponding to the pyoglutamate residue of the added GSH moiety; Baillie and Davis, 1993). The MS^2 spectrum also showed fragment ions at m/z 283, which corresponded to the cleavage of the C—S bond of the cysteine residue of GSH moiety that is conjugated to DPH.

The fragment ion at m/z 383 derived from GSH-conjugated benzene was derived from the DPH moiety. The fragment ion at m/z 272 and 254 corresponded to the cleavage of the C—S bond of cysteine residue of GSH moiety and GSH conjugated with benzene derived from DPH, which lost the pyoglutamate residue of the added GSH moiety, respectively. The fragment ion at m/z 210 corresponded to the cleavage of the hydantoin of DPH, which was conjugated with sulfur in the benzene moiety. This observation was most likely caused by the cleavage of the C—S bond of the cysteine residue of GSH moiety as previously described. The

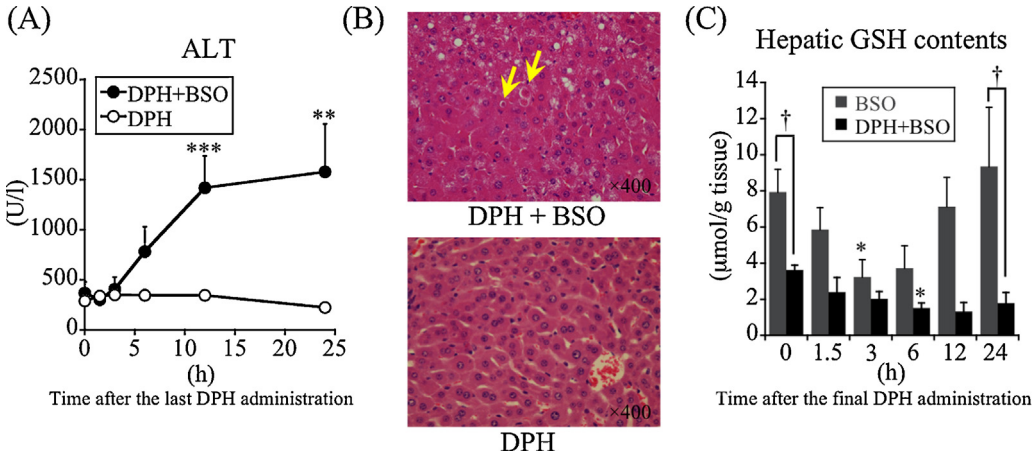

Fig. 1. Effects of BSO treatment on DPH-induced liver injury in mice. The mice were intraperitoneally administered DPH at a dose of 50 mg/kg for 2 days followed by oral administration of 100 mg/kg DPH on days 3 through 5. BSO (700 mg/kg) was intraperitoneally injected 1 h prior to each DPH administration. At 0, 1.5, 3, 6, 12, and 24 h after the final DPH administration, blood was collected to measure the plasma ALT levels (A). Hematoxylin and eosin (H&E) staining was performed on liver sections from 24 h after the final DPH treatment (B). The arrows indicate apoptotic cells. The hepatic GSH contents were measured at 0, 1.5, 3, 6, 12, 24 h after the final DPH administration. Data are shown as the mean ± SE of the results from 6 to 12 mice. The differences compared with the mice administered DPH alone were considered significant at $^{**}P < 0.01$ and $^{***}P < 0.001$ (A). The differences compared with 0 h were considered significant at $^{*}P < 0.05$, and the differences compared with BSO alone-treated mice were considered significant at $\dagger P < 0.05$ (C).

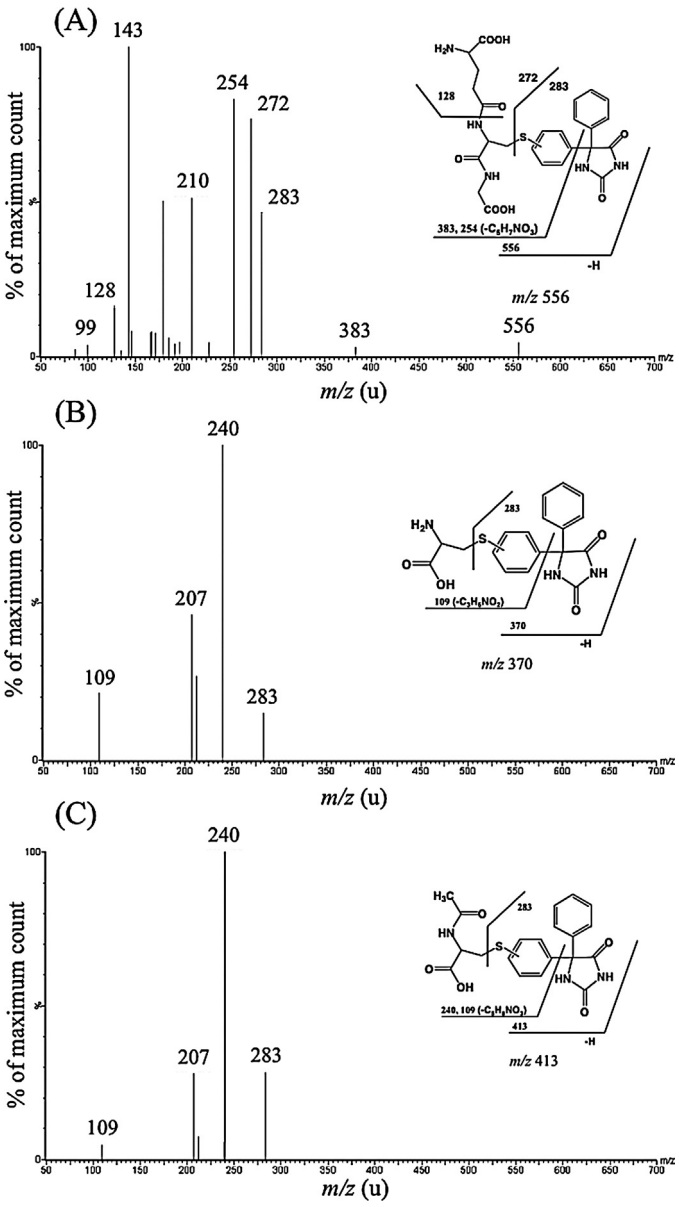

Fig. 2. LC–MS/MS analyses of GS-DPH adduct in bile (A), and Cys- (B) or NAC-DPH (C) adducts in the plasma of mice with DPH-induced liver injury. The mice were intraperitoneally administered DPH at a dose of 50 mg/kg for 2 days followed by oral administration of 100 mg/kg DPH on days 3 through 5. The bile was collected at 3–6 h after the final DPH administration (A). Bile was pooled from 4 mice and used for LC–MS/MS analysis (A). The plasma was collected 24 h after the final DPH administration (B and C). MS spectrum of the parent M^- ion *m/z* 556 (A), *m/z* 370 (B) and *m/z* 413 (C) were observed at 9.8, 9.7 and 10.7 min of the elution time, respectively. The product ion spectrum of the each of parent M^- ion was detected in the bile (A) and plasma (B and C).

structural feature consists of the attachment of GSH to the benzoic moiety of DPH, with a conjugation occurring at the benzene portion of drug (Fig. 2A). Taken together, a nucleophilic attack on the arene oxide intermediate by GSH followed by dehydration would result in the formation of the identified GSH adduct. We proposed that a potential mechanism for the metabolic activation of DPH would involve epoxidation of the benzene residues to form well-known reactive metabolites as an arene oxide intermediate (Fig. 6).

In plasma, Cys-DPH (*m/z* 370) and NAC-DPH (*m/z* 413) were detected, and the extracted ion chromatogram showed a peak at 10.7 min and 9.7 min of elution time, respectively (Fig. 2A and B). The mass of the molecular ion of Cys-DPH (*m/z* 370) suggested an addition of 121 Da to the mass of DPH, which corresponded to the addition of cysteine molecules (Fig. 2B), and the molecular ion of NAC-DPH (*m/z* 412) suggested an addition of 163 Da to the mass of DPH (*m/z* 251), which corresponded to the addition of NAC molecules (Fig. 2C). The MS^2 spectrum of both Cys-DPH and NAC-DPH showed fragment ions at *m/z* 283, which corresponded to the cleavage of the C—S bond of the cysteine residue of the cysteine or NAC moiety. The fragment ion at *m/z* 109 derived from sulfur-conjugated benzene of the DPH moiety was most likely formed by the cleavage of the C—S bond of the cysteine residue of GSH following GSH conjugation to DPH in the benzene moiety. The structural feature consisted of the attachment of cysteine or NAC to the benzoic moiety of DPH. Considering these observations, the Cys-DPH and NAC-DPH adducts most likely were derived from the corresponding GS-DPH adducts *via* the mercapturic acid pathway and may be a reflection of the formation of the arene oxide intermediate *in vivo*.

3.3. Effects of DPH administration on the expression levels of Cyp2c and Cyp3a protein and enzyme activities in mouse liver microsomes

In our mouse model, DPH-induced liver injury was developed by repetitive DPH and BSO co-administration. Thus, changes of hepatic P450 protein contents and activities were hypothesized to contribute to the onset of liver injury. To investigate the effects of DPH administration on the hepatic P450, microsomal Cyp2c and Cyp3a protein contents and its enzyme activities were assessed. It has been reported that inflammation affects P450 protein contents and its enzyme activities. (Morgan, 1993; Shedlofsky et al., 1994). Thus, we assessed hepatic P450 contents and related enzyme activities until on day 4 of the repeated DPH administration. On days 0, 1, 2, and 4, liver microsomes were obtained. Both the hepatic Cyp2c and Cyp3a protein contents were significantly increased on days 1–4 compared with those on day 0 and were increased in a dose-dependent manner (Fig. 3A). The TOL hydroxylation activities were significantly increased on days 1–4 compared with those on day 0 and were increased in a dose-dependent manner (Fig. 3B). The MDZ hydroxylation activity was significantly decreased on days 2–4 compared with that on day 0 (Fig. 3B). These results suggested that modulation of P450 protein expression and its activity, especially Cyp2c induction was involved in the onset of DPH-induced liver injury.

3.4. Time-dependent changes of concentration of plasma DPH and its thiol conjugates

To confirm formation of the arene oxide intermediate in the DPH-induced liver injury, time-dependent changes of the plasma concentration of DPH and plasma levels of Cys-DPH or NAC-DPH on day 3 and day 5, which corresponded to non-liver injury and liver injury conditions, respectively, were analyzed. At 0, 1.5, 3, 6, 12, and 24 h after DPH administration on day 3 and day 5, blood was collected and the plasma concentration of each metabolite was analyzed using the LC–MS/MS system. MS/MS data acquisition was performed with the electrospray source operating in the negative or positive mode (ESIneg or ESIpos) under MRM conditions as shown in Table 1. On day 5, the plasma concentration of DPH peaked at 3 h after the final administration and then slowly decreased (Fig. 4). Furthermore, on day 5, Cys-DPH and NAC-DPH adducts were detected and increased in a time-dependent manner (Fig. 4). However, on day 3, when liver injury had not occurred, Cys-DPH and NAC-DPH could not be detected. The thiol conjugate level in plasma was well correlated with increases of the plasma ALT levels in the individual animals (643, 691, 983, and 1764 of the relative level of plasma NAC-DPH *vs.* 413, 576, 2740, and 3040 U/l of

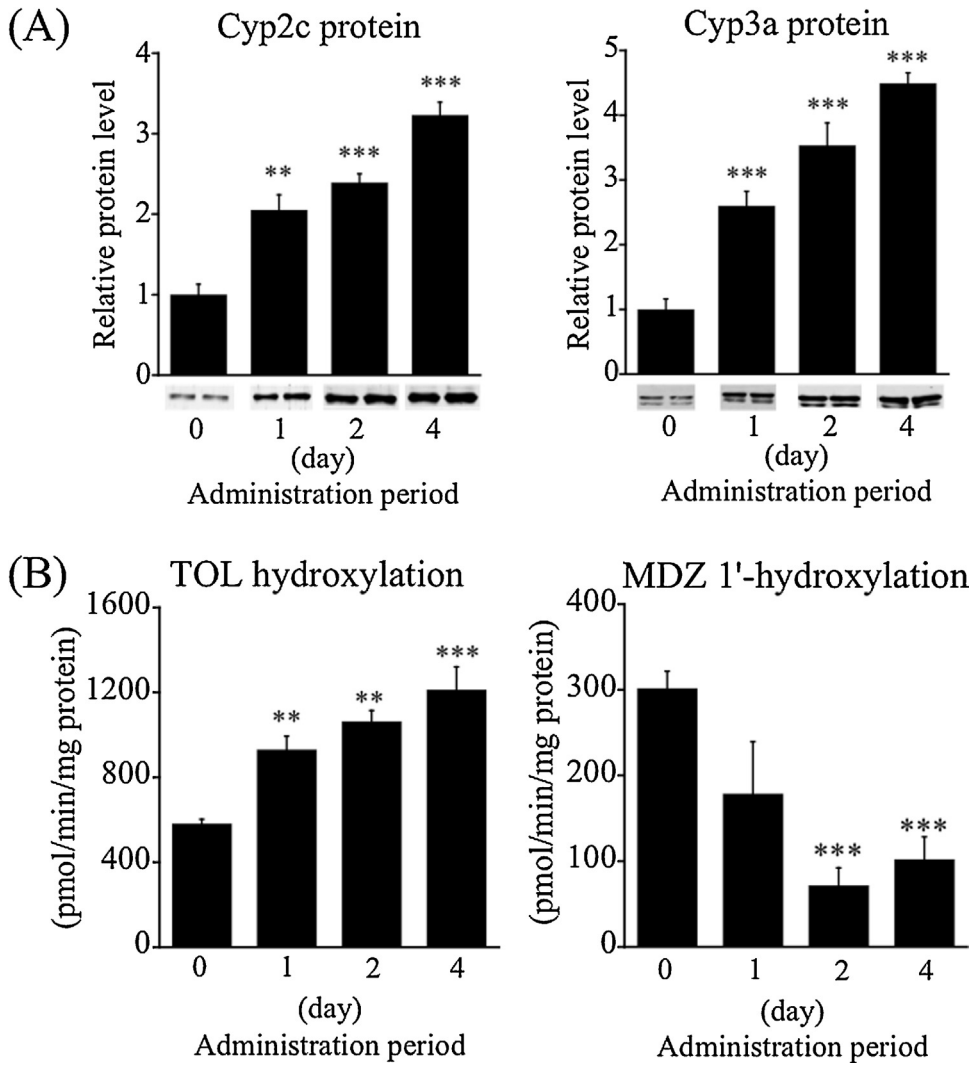

Fig. 3. Effects of DPH administration on the expression levels of Cyp2c and Cyp3a protein and its enzyme activities. The mice were intraperitoneally administered DPH at a dose of 50 mg/kg for 2 days followed by oral administration of 100 mg/kg DPH on days 3 and 4. Mouse liver microsomes were prepared 24 h after the 0, 1, 2, and 4 times of DPH administration. Microsomal Cyp2c and Cyp3a protein contents were assessed by immunoblotting analysis. Quantitative analysis of protein expression was performed using a densitogram (A). Microsomal Cyp2c and Cyp3a activities were evaluated by TOL hydroxylation and MDZ 1′-hydroxylation, respectively, using HPLC (B). The data are shown as the mean ± SE of the results from 4 to 5 mice. The differences compared with the non-treated mice (Day 0) were considered significant at $^{**}P < 0.01$ and $^{***}P < 0.01$. N.D.: not detected.

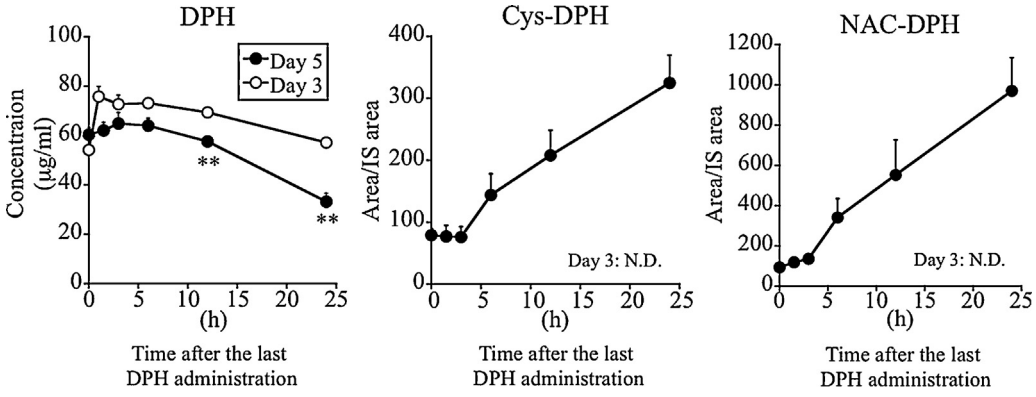

Fig. 4. Changes in the plasma concentration of DPH and its thiol-conjugated metabolites in mice with DPH-induced liver injury. The mice were intraperitoneally administered DPH at a dose of 50 mg/kg for 2 days followed by oral administration of 100 mg/kg DPH on days 3 through 5. BSO (700 mg/kg) was intraperitoneally injected 1 h prior to each DPH administration. At 0, 1.5, 3, 6, 12, and 24 h after the 3 times of DPH administration (indicated as day 3, without liver injury) and after the final DPH administration (indicated as day 5, with liver injury), blood was collected for the assessment of DPH and its thiol conjugates in plasma. The data are shown as the mean ± SE of the results obtained from 6 to 12 mice. In the case of DPH, the differences compared with the plasma concentrations on day 3 at each time points were considered significant at $^{**}P < 0.01$. N.D.: not detected.

plasma ALT level, respectively). These results suggested that the arene oxide intermediate was involved in the development of DPH-induced liver injury in mice.

3.5. Effects of P450 inhibitor on DPH-induced liver injury in mice

To investigate whether metabolites formed by P450-mediated metabolism were involved in DPH-induced liver injury, the mice were treated with ABT, a non-selective P450 inhibitor, 1 h prior to the final DPH administration and the plasma ALT levels, plasma thiol conjugates levels, and the hepatic GSH contents were analyzed. The plasma ALT levels were significantly decreased by ABT treatment 24 h after the final DPH administration (Fig. 5A). The hepatic GSH content at 24 h after the final DPH treatment was measured. We found that ABT treatment significantly restored the hepatic GSH contents in mice treated with both DPH and BSO compared with non-ABT-treated mice (Fig. 5B). Furthermore, ABT alone treatment did not affect the hepatic GSH contents (Fig. 5B). These results suggested that the inhibition of P450-mediated metabolism suppressed the development of DPH-induced liver injury.

To assess whether changes in the thiol conjugates formations are involved in the effects of ABT treatment on DPH-induced hepatotoxicity, we performed analyses of the time-dependent changes of the plasma DPH concentration and its thiol conjugates levels in DPH-induced liver injury mice with or without ABT treatment. The plasma concentrations of DPH were significantly increased in ABT-treated mice compared with vehicle-treated (-ABT) mice (Fig. 5C). In the plasma, NAC-DPH was significantly decreased at 24 h after the final DPH administration, whereas Cys-DPH was significantly decreased at all time points by the ABT treatment (Fig. 5C). These results suggest that the arene oxide intermediate formed by P450-mediated metabolism was inhibited by ABT treatment that would contribute to restore the hepatic GSH contents in mice. Considering these observations, under the GSH-decreased condition, the arene oxide intermediate formed by the P450-mediated metabolisms would be a hepatotoxic metabolite rather than the parent drug.

4. Discussion

Recently, we have established a mouse model of DPH-induced liver injury (Sasaki et al., 2013). In this model, the liver injury was exacerbated by the co-administration with BSO, which suggested that GSH has a crucial protective role for DPH-induced liver injury (Fig. 1A). BSO is a specific inhibitor of γ-GCS, a rate-limiting enzyme of GSH synthesis (Griffith and Meister, 1979). In addition, it has been reported that BSO has no effect on the content and function of microsomal P450s and conjugating enzymes, such as GSH *S*-transferase, sulfotransferase, and UDP-glucuronosyltransferase (UGT) (Drew and Miners, 1984; Watanabe et al., 2003). A number of groups, including our group, have applied GSH-depleted animal models to the evaluation of hepatotoxic potential for several drugs that produce reactive metabolites, for example acetaminophen (Watanabe et al., 2003), methimazole (Kobayashi et al., 2012), amodiaquine (Shimizu et al., 2009), and ticlopidine (Shimizu et al., 2011). Taken together, we considered that GSH-trapped metabolites are involved in DPH-induced liver injury.

The formation of thiol conjugates of DPH has been previously suggested by *in vitro* studies (Roy and Snodgrass, 1988, 1990).

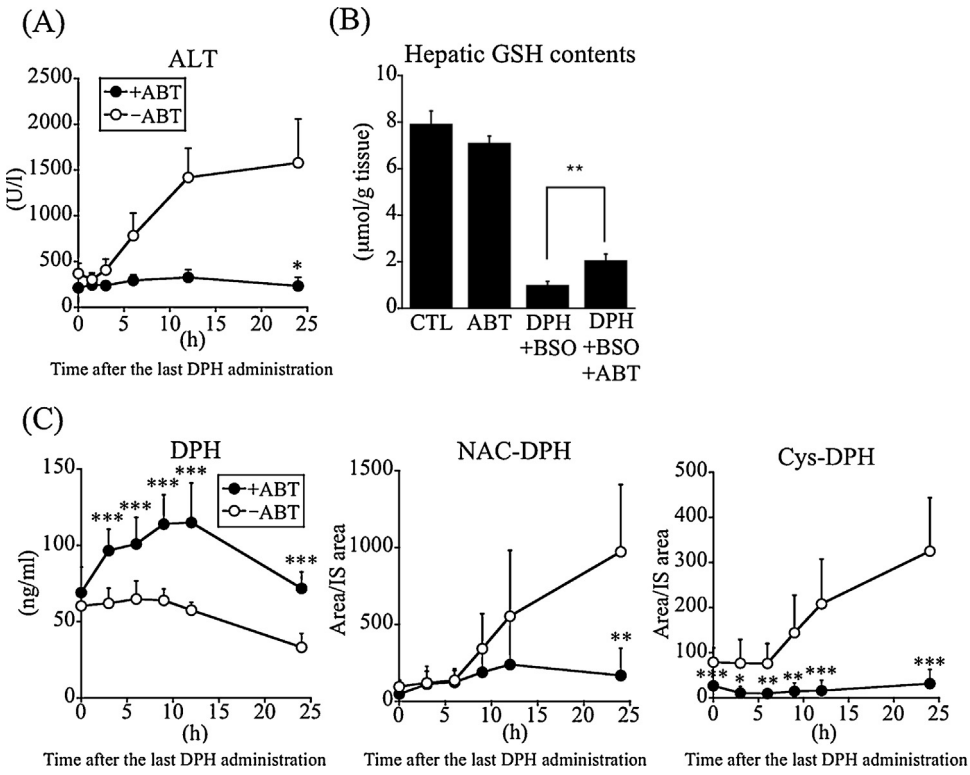

Fig. 5. Effects of ABT treatment on mice with DPH-induced liver injury. The mice were intraperitoneally administered DPH at a dose of 50 mg/kg for 2 days followed by oral administration of 100 mg/kg DPH on days 3 through 5. BSO (700 mg/kg) was intraperitoneally injected 1 h prior to each DPH administration. ABT (100 mg/kg), a non-specific inhibitor of P450, was intraperitoneally administered 1 h prior to the final DPH administration. At 0, 3, 6, 9, 12, and 24 h after the final DPH administration, blood was collected for measuring the plasma ALT levels (A) and DPH and its thiol conjugates concentrations (C). The livers were collected at 24 h after the final DPH administration to measure the hepatic GSH contents (B). The data are shown as the mean ± SE of the results obtained from 4 to 12 mice. The differences compared with non-ABT-treated mice at each time point were considered significant at $^{*}P < 0.05$, $^{**}P < 0.01$ and $^{***}P < 0.001$ (A and C), and the differences compared with the non-ABT-treated mice were considered significant at $^{**}P < 0.01$ (B).

Therefore, the formation of GS-DPH adducts is also plausible *in vivo*. However, thiol conjugates of DPH-derived intermediates have not been previously identified *in vitro* and *in vivo*. In the present study, the GS-DPH adduct of the putative arene oxide intermediate was detected in bile collected from mice with DPH-induced liver injury utilizing LC–MS/MS analysis (Fig. 2A). Furthermore, Cys- or NAC-DPH adduct of the putative arene oxide intermediate were also detected in the plasma collected from mice with DPH-induced liver injury (Fig. 2B and C). These thiol-DPH adducts are considered to be the subsequent products of the arene oxide intermediate produced by GSH conjugation (Fig. 6). At 0 h to 24 h after the final DPH administration, the formation of plasma Cys- or NAC-DPH adducts were time-dependently increased (Fig. 4) with corresponding lower levels in the hepatic GSH contents (Fig. 1C). Considering these observations, hepatic GSH would be consumed for conjugation with the electrophilic arene oxide intermediate, resulting in a decreased hepatic GSH contents (Fig. 1C) and suggesting that GS-DPH adducts can be converted into the corresponding Cys-DPH and NAC-DPH adducts *via* the mercapturic acid pathway (Meister and Anderson, 1983). In addition, we hypothesize that the arene oxide intermediate which would be converted into GS-, Cys-, or NAC-DPH adducts not only form these thiol conjugates, but also could put stress on the hepatocyte *via* cellular dysfunction, namely as electrophilic stress (Takakusa et al., 2008). Moreover, it would appear that if hepatic GSH is decreased by conjugation of the arene oxide intermediate or GSH depletion reagent such as BSO, the arene oxide intermediate could escape from GSH conjugation leading to increased reaction of the arene oxide intermediate with cellular molecules that would put hepatocyte into cellular dysfunction. The products, formed by the reaction with the arene oxide intermediate and cellular molecules, may be recognized as a foreign antigen, leading to an immune-mediated liver injury as previously reported (Sasaki et al., 2013).

The arene oxide intermediate formation, which can be converted into thiol conjugates, was suggested for the development of DPH-induced liver injury (Fig. 4). As shown in Fig. 4, we could detect the thiol conjugates of DPH in mice only at day 5 but not in day 3, which corresponded to non-hepatotoxic conditions (Sasaki et al., 2013). This result strongly supports the concept that formation of the arene oxide intermediate is critical for developing the liver injury. In fact, with the increases of relative levels of the plasma these thiol conjugates were well correlated with the elevation of plasma ALT level in the 4 individual animals (Fig. 4).

In the present study, we found that P450-mediated metabolisms were involved in hepatotoxicity and hepatic GSH decrease by DPH administration. Co-treatment of ABT, a non-selective P450 inhibitor, significantly suppressed the development of

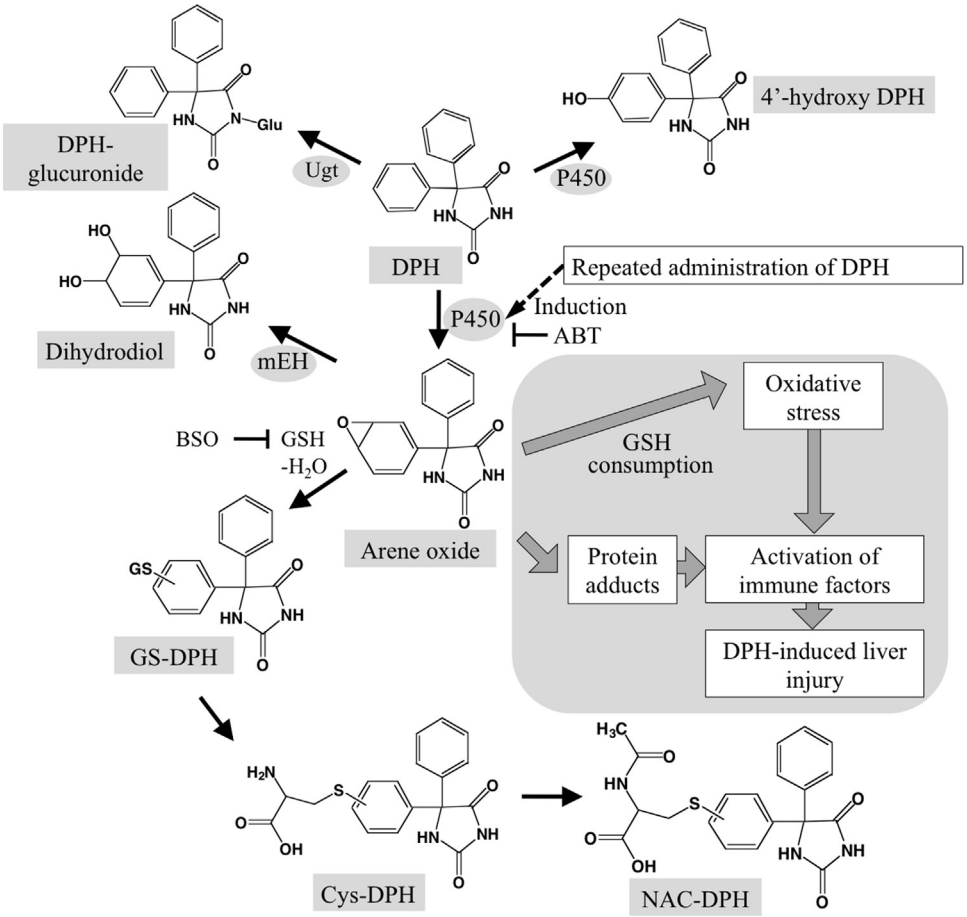

Fig. 6. Putative metabolic pathway of DPH from our results combined with previous reports (Maguire 1988; Szabo et al., 1990). In the present study, GS-DPH, Cys-DPH, and NAC-DPH adducts derived from the arene oxide intermediate are detected *in vivo*, and BSO treatment exacerbated DPH-induced liver injury suggesting the arene oxide intermediate is partially detoxified by GSH conjugation. *In vivo* P450 inhibition studies shown that the arene oxide intermediate was formed by P450-mediated metabolism. P450 protein expression and activities are modulated by the repeated exposure of DPH in mice that might be critical for the arene oxide intermediate formation. GSH depletion agent exacerbated the DPH-induced liver injury *via* decreased GSH conjugation to the arene oxide intermediate. This event would be causal for the electrophilic stress and oxidative stress followed by hepatic lesion may lead to the immune- and inflammation-mediated DPH-induced liver injury as previously reported (Sasaki et al., 2013). Glu.: glucuronic acid.

DPH-induced liver injury (Fig. 5A) in association with a reduction in the plasma concentrations of Cys-DPH and NAC-DPH adducts (Fig. 5C), thereby restoring the hepatic GSH content (Fig. 5B). These results suggested that P450-mediated metabolic activation, formation of the arene oxide intermediate, is critical for the development of DPH-induced liver injury.

As described above, Cys-DPH and NAC-DPH adducts were only detected on day 5 but not on day 3 (Fig. 4). At the same time, P450 was induced in a dosing period-dependent manner (Fig. 3A). Therefore, we speculated that P450 induction is involved to develop DPH-induced liver injury. In addition, we assumed that P450 induction by the repetitive exposure of DPH for 3 days could not form sufficiently of the arene oxide intermediate to generate electrophilic stress. In fact, plasma thiol conjugates were not observed on day 3 (Fig. 4). Taken together, the hepatotoxic potential of DPH is affected by the hepatic P450 induction. This concept is supported by the previous study showing that the single administration of DPH, which is close to the amount of LD_{50}, failed to develop the liver injury even combination with BSO treatment in mice (Sasaki et al., 2013).

It has been suggested that arene oxide intermediate is only formed in mouse but not in human microsomes as reported by Riley et al. (1988). In addition, although the cytotoxicity by murine microsomal enzyme-dependent DPH metabolism was significantly enhanced by the epoxide hydrolase inhibitor, trichloropropane oxide (TCPO), treatment, no significant enhancement of cytotoxicity was observed in the presence of human liver microsomes (Riley et al., 1988). These observations suggest that arene oxide-mediated toxicity is not involved with DPH-induced liver injury in human. However, the dihydrodiol form of DPH in the urine of newborn human infants was reported by Horning et al. (1971). By analogy with the formation of dihydrodiols from known epoxides, it is considered that the arene oxide intermediate might be involved in DPH metabolism *in vivo* in human (Glazko, 1973). In the present study, we suggested that P450 induction was critical for enhancement of the arene oxide intermediate formation in mice (Figs. 3 and 4). Therefore, P450 induction followed by enhancement of the arene oxide intermediate formation might be critical for the arene oxide-mediated toxicity in human. However, there was no report that P450 induction was related to the formation of the arene oxide intermediate in human.

In conclusion, for the first time, this study identified a novel putative GSH conjugate of the arene oxide intermediate of DPH and provided evidence that DPH bioactivation by P450 and hepatic GSH may play an important role in the development of DPH-induced liver injury. These postulated mechanisms are summarized in Fig. 6. These observations provide insight into the metabolic activation-based mechanisms of drug-induced liver injury and may help to assess the reactive metabolite-mediated toxicity in drug development.

Funding information

We obtained funding from the Health and Labor Sciences Research Grants from the Ministry of Health, Labor, and Welfare of Japan (H23-BIO-G001).

Conflict of interest

None of the authors have any conflicts of interest related to this manuscript.

Transparency document

The Transparency document associated with this article can be found in the online version.

Acknowledgments

We thank Miss Azumi Iida and Mr. Kentaro Matsuo for their excellent technical assistance in the animal treatments and sample preparations.

References

Baillie, T.A., Davis, M.R., 1993. Mass spectrometry in the analysis of glutathione conjugates. Biol. Mass Spectrom. 22, 319–325.
Chaudhry, A.S., Urban, T.J., Lamba, J.K., Birnbaum, A.K., Remmel, R.P., Subramanian, M., Strom, S., You, J.H., Kasperaviciute, D., Catarino, C.B., et al., 2010. CYP2C9*1B promoter polymorphisms, in linkage with CYP2C19*2, affect phenytoin autoinduction of clearance and maintenance dose affect phenytoin autoinduction of clearance and maintenance dose. J. Pharmacol. Exp. Ther. 332, 599–611.
Drew, R., Miners, J.O., 1984. The effects of buthionine sulphoximine (BSO) on glutathione depletion and xenobiotic biotransformation. Biochem. Pharmacol. 33, 2989–2994.
Emoto, C., Yamazaki, H., Yamasaki, S., Shimada, N., Nakajima, M., Yokoi, T., 2000. Characterization of cytochrome P450 enzymes involved in drug oxidations in mouse intestinal microsomes. Xenobiotica 30, 943–953.
Fleishaker, J.C., Pearson, L.K., Peters, G.R., 1995. Phenytoin causes a rapid increase in 6β-hydroxycortisol urinary excretion in humans – a putative measure of CYP3A induction. J. Pharm. Sci. 84, 292–294.
Glazko, A.J., 1973. Diphenylhydantoin metabolism. A prospective review. Drug Metab. Dispos. 5, 711–714.
Griffith, O.W., Meister, A., 1979. Potent and specific inhibition of glutathione synthesis by buthionine sulfoximine (*S-n*-butyl homocysteine sulfoximine). J. Biol. Chem. 254, 7558–7560.
Hagemeyer, C.E., Bürck, C., Schwab, R., Knoth, R., Meyer, R.P., 2010. 7-Benzyloxyresorufin-*O*-dealkylase activity as a marker for measuring cytochrome P450CYP3A induction in mouse liver. Anal. Biochem. 398, 104–111.
Haruda, F., 1979. Phenytoin hypersensitivity: 38 cases. Neurology 11, 1480–1485.
Horning, M.G., Stratton, C., Wilson, A., Horning, E.C., Hill, R.M., 1971. Detection of 5-(3,4-dihydroxy-1,5-cyclohexadien-1-yl)-5-phenylsydantoin as a major metabolite of 5,5-diphenylhydantoin (Dilantin) in the newborn human. Anal. Lett. 4, 537–545.
Kitamura, S., Maeda, K., Wang, Y., Sugiyama, Y., 2008. Involvement of multiple transporters in the hepatobiliary transport of rosuvastatin. Drug Metab. Dispos. 36, 2014–2023.
Kobayashi, M., Higuchi, S., Ide, M., Nishikawa, S., Fukami, T., Nakajima, M., Yokoi, T., 2012. Th2 cytokine-mediated methimazole-induced acute liver injury in mice. J. Appl. Toxicol. 32, 823–833.
Laemmli, U.K., 1970. Cleavage of structural proteins during the assembly of the head of bacteriophage T4. Nature 227, 680–685.
Maguire, J.H., 1988. Quantitative estimation of catechol/methylcatechol pathways in human phenytoin metabolism. Epilepsia 29, 753–759.
Meister, A., Anderson, M.E., 1983. Glutathione. Annu. Rev. Biochem. 52, 711–760.
Morgan, E.T., 1993. Down-regulation of multiple cytochrome P450 gene products by inflammatory mediators *in vivo*: independence from the hypothalamo-pituitary axis. Biochem. Pharmacol. 45, 415–419.
Mugford, C.A., Mortillo, M., Mico, B.A., Tarloff, J.B., 1992. 1-Aminobenzotriazole-induced destruction of hepatic and renal cytochromes P450 in male Sprague-Dawley rats. Fundam. Appl. Toxicol. 19, 43–49.
Mullick, F.G., Ishak, K.G., 1980. Hepatic injury associated with diphenylhydantoin therapy. A clinicopathologic study of 20 cases. Am. J. Clin. Pathol. 4, 442–452.
Riley, R.J., Maggs, J.L., Lambert, C., Kitteringham, N.R., Park, B.K., 1988. An *in vitro* study of the microsomal metabolism and cellular toxicity of phenytoin: sorbinil and mianserin. Br. J. Clin. Pharmacol. 5, 577–588.
Roy, D., Snodgrass, W.R., 1988. Phenytoin metabolic activation: role of cytochrome P-450 glutathione, age, and sex in rats and mice. Res. Commun. Chem. Pathol. Pharmacol. 59, 173–190.
Roy, D., Snodgrass, W.R., 1990. Covalent binding of phenytoin to protein and modulation of phenytoin metabolism by thiols in A/J mouse liver microsomes. J. Pharmacol. Exp. Ther. 252, 895–900.
Sasaki, E., Matsuo, K., Iida, A., Tsuneyama, K., Fukami, T., Nakajima, M., Yokoi, T., 2013. A novel mouse model for phenytoin-induced liver injury: involvement of immune-related factors and p450-mediated metabolism. Toxicol. Sci. 136, 250–263.
Shedlofsky, S., Israel, B.C., McClain, C.J., Hill, D.B., Blouin, R.A., 1994. Endotoxin administration to humans inhibits hepatic cytochrome P450-mediated drug metabolism. J. Clin. Invest. 94, 2209–2214.
Shimizu, S., Atsumi, R., Itokawa, K., Iwasaki, M., Aoki, T., Ono, C., Izumi, T., Sudo, K., Okazaki, O., 2009. Metabolism-dependent hepatotoxicity of amodiaquine in glutathione-depleted mice. Arch. Toxicol. 83, 701–707.
Shimizu, S., Atsumi, R., Nakazawa, T., Izumi, T., Sudo, K., Okazaki, O., Saji, H., 2011. Ticlopidine-induced hepatotoxicity in a GSH-depleted rat model. Arch. Toxicol. 85, 347–353.
Spielberg, S.P., Gordon, G.B., Blake, D.A., Goldstein, D.A., Herlong, H.F., 1981. Predisposition to phenytoin hepatotoxicity assessed in vitro. N. Engl. J. Med. 305, 722–727.

Szabo, G.K., Pylilo, R.J., Davoudi, H., Browne, T.R., 1990. Simultaneous determination of *p*-hydroxylated and dihydrodiol metabolites of phenytoin in urine by high-performance liquid chromatography. J. Chromatogr. 535, 279–285.

Takakusa, H., Masumoto, H., Mitsuru, A., Okazaki, O., Sudo, K., 2008. Markers of electrophilic stress caused by chemically reactive metabolites in human hepatocytes. Drug Metab. Dispos. 36, 816–823.

Tietze, F., 1969. Enzymic method for quantitative determination of nanogram amounts of total and oxidized glutathione: applications to mammalian blood and other tissues. Anal. Biochem. 27, 502–522.

Watanabe, T., Sagisaka, H., Arakawa, S., Shibaya, Y., Watanabe, M., Igarashi, I., Tanaka, K., Totsuka, S., Takasaki, W., Manabe, S., 2003. A novel model of continuous depletion of glutathione in mice treated with L-buthionine (S,R)-sulfoximine. J. Toxicol. Sci. 5, 455–469.

Yamazaki, H., Komatsu, T., Takemoto, K., Saeki, M., Minami, Y., Kawaguchi, Y., Shimada, N., Nakajima, M., Yokoi, T., 2001. Decreases in phenytoin hydroxylation activities catalyzed by liver microsomal cytochrome P450 enzymes in phenytoin-treated rats. Drug Metab. Dispos. 29, 427–434.